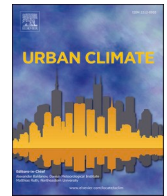




ELSEVIER

Contents lists available at [ScienceDirect](https://www.sciencedirect.com)

Urban Climate

journal homepage: www.elsevier.com/locate/uclim

Response characteristics and influencing factors of carbon emissions and land surface temperature in Guangdong Province, China

Chunrui Song^a, Jun Yang^{a,b,c,*}, Feng Wu^{d,**}, Xiangming Xiao^e, Jianhong Xia (Cecilia)^f, Xueming Li^a

^a Human Settlements Research Center, Liaoning Normal University, 116029 Dalian, China

^b School of Humanities and Law, Northeastern University, Shenyang 116029, China

^c Jangho Architecture College, Northeastern University, Shenyang 110169, China

^d Key Laboratory of Regional Sustainable Development Modeling, Institute of Geographic Sciences and Natural Resources Research, CAS, Beijing 100101, China

^e Department of Microbiology and Plant Biology, Center for Earth Observation and Modeling, University of Oklahoma, Norman, OK 73019, USA

^f School of Earth and Planetary Sciences (EPS), Curtin University, Perth 65630, Australia

ARTICLE INFO

Keywords:

Carbon emissions

LST

Spearman correlation analysis

Geodetector

Influencing factors

Sustainable development

ABSTRACT

The continuous rise of carbon emissions has brought enormous pressure on the human environment. To determine the response characteristics and influencing factors of carbon emissions and land surface temperature (LST), we used the land use, LST, carbon emissions, and socio-economic data of Guangdong Province in 2000, 2005, 2010, and 2017 through Spearman correlation analysis and factor detection of Geodetector. The findings revealed that carbon emissions had a semi-circular hierarchical structure from 2000 to 2017. The areas with significant carbon emissions were distributed in some counties and districts of Zhongshan, Dongguan, Guangzhou, and Shenzhen, and they continued to increase and expand outward. The annual average LST in Guangdong Province is between 17 and 24 °C, and the average daytime and nighttime LST are 21–28 °C and 13–20 °C, respectively. Total carbon emissions and LST have a positive coefficient of 0.3–0.7. The leading factors of carbon emissions in Guangdong Province are different in different periods, but the influence of economic aggregate (GRP), land scale (LS), and land intensity (LI) on the spatial differentiation of carbon emissions is relatively strong. The interaction effect of factors is more significant than the single factors. The outcome of the study is valuable for decision-makers to formulate emission reduction policies and achieve sustainable urban development.

1. Introduction

Rapid economic development and anthropogenic activities have increased carbon dioxide emissions, with the associated

* Corresponding author at: Human Settlements Research Center, Liaoning Normal University, 116029 Dalian, China.

** Corresponding author.

E-mail addresses: yangjun8@mail.neu.edu.cn (J. Yang), wufeng@igsrr.ac.cn (F. Wu), xiangming.xiao@ou.edu (X. Xiao), c.xia@curtin.edu.au (J. Xia).

<https://doi.org/10.1016/j.uclim.2022.101330>

Received 12 September 2022; Received in revised form 5 October 2022; Accepted 19 October 2022

Available online 26 October 2022

2212-0955/© 2022 Elsevier B.V. All rights reserved.

environmental problems becoming more prominent. Chinese carbon emissions surpassed the America in 2007, making China become the world's largest carbon emitter (Gregg et al., 2008). Facing enormous pressure to reduce emissions, China and several other countries established two main targets for reducing emissions: first, to peak carbon emissions by 2030, and second, to strive to achieve carbon neutrality by 2060 (Zhao et al., 2022; Zou et al., 2021). Current research on carbon emissions focuses on carbon budget, carbon transfer, carbon emission intensity simulation, accurate assessment, future prediction (Acheampong and Boateng, 2019; Dong et al., 2018; Zhou et al., 2021), and the spatiotemporal evolution and influencing factors of carbon emissions at different scales (Cao and Yuan, 2019; Wang et al., 2022). According to the study of Zhou et al., the relationship between urbanization and land use carbon emissions in the Beijing-Tianjin-Hebei region can be summarized into three modes: "high urbanization-low emissions," "moderate urbanization-high emissions," and "low urbanization-low emissions"; however, the polycentric structure of some urban agglomerations do not achieve the effect of carbon emission reduction to a certain extent, but instead promotes carbon emission (Wang et al., 2022; Zhou et al., 2021). For China, population size has the highest sensitivity weight to carbon emission intensity (Acheampong and Boateng, 2019). Carbon emission influencing factors are closely related to human activities and include fossil energy consumption, economic development, urban spatial form, urban transportation, policies, cement production, and land use (Chen et al., 2022; Dumortier and Elobeid, 2021; Lin and Benjamin, 2017; Sun et al., 2022; Yang et al., 2021b). Among these, Zhang et al. showed that the carbon emissions from fossil energy consumption in Shandong Province account for 70–80% of the total carbon emissions (Zhang et al., 2017), and Huang et al. took the global as the study area and showed that carbon dioxide emissions from construction industry accounted for 23% of carbon dioxide emissions from economic activities (Chen et al., 2017; Huang et al., 2018). Studies have also focused on reducing and suppressing the total amount of ever-increasing carbon emissions. Results show that the terrestrial ecosystems in China have a huge capacity for carbon sequestration (Li et al., 2021a; Xu et al., 2019). Furthermore, studies have marked that the interaction between new and fossil energy indirectly promotes fossil energy consumption and carbon emissions (Cang et al., 2021). A country's different economic development stages also affect the relationship between its energy consumption and carbon emissions (Waheed et al., 2019).

Climate change is one of the most challenging research topics during the last few decades, as temperature rise has already posed a significant impact on the earth's functions (Cartalis et al., 2015; Eleftheriou et al., 2018). In the early 19th century, Howard (1833) initiated the first study on urban heat islands in London and its suburbs by observing and recording the surface temperatures. LST, the ground temperature measured by thermal radiation, is also a key variable in climate research. (de Almeida et al., 2021; Sekertekin and Zadbagher, 2021; Yang et al., 2021a). Several factors, such as the properties of the underlying surface, impervious surface, building layout, anthropogenic heat source emissions, wind speed, cloud cover, and aerosols, influence the LST, either individually or in combination (Cui et al., 2016; Shi et al., 2022; Wang et al., 2018; Yang et al., 2020, 2021c; Zhao et al., 2021). Among them, Normalized Difference Built-up Index (NDBI) and Normalized Difference Vegetation Index (NDVI) are determined to be highly correlated indices of LST (Sekertekin and Zadbagher, 2021). Early research methods, relying on LST data obtained mainly from station observations, have considerable limitations, especially in reflecting temperature variations over large areas (Muchoney and Strahler, 2002; Norman et al., 1995). Remote sensing observation can monitor temperatures simultaneously over a large area, so studies combining the observations from remote sensing and station monitoring have great advantages (Li et al., 2021b; Zhang and Xu, 2020). Commonly used quantitative inversion algorithms for LST include single-channel, split-window, and multi-channel (Ghorbannia et al., 2017; Rongali et al., 2018; Zhong et al., 2015). Major directions of research concerning LST include temporal and spatial changes and influencing factors of LST, LST monitoring data and quantitative inversion, and prediction of urban heat islands with simulations (Li and Zhang, 2021; Nakata-Osaki et al., 2018; Parvez et al., 2021; Ren et al., 2022). The cellular automata (CA) algorithm is widely used in simulation research of urban heat islands, but the model methods selected for different scales are distinct. For example, Weather Research and Forecasting (WRF) and computational fluid dynamics (CFD) models are often utilized in mesoscale research, while ENVI-met model is more suitable for microclimate simulation (Cortes et al., 2022; Wagner et al., 2015; Wang and Li, 2016). In recent years, climate problems such as high temperature and extreme weather occur frequently (He et al., 2021, 2022). More and more scholars pay attention to the impact of carbon emissions and realize the response mechanism between carbon emissions and LST. And the research is mostly based on the impact of land cover on carbon emissions. For example, Kafy et al. evaluated the impact of vegetation loss on carbon emissions and LST (Kafy et al., 2022; Rahaman et al., 2022); Fattah et al. used artificial neural networks to model future the impact of land-specific carbon emission patterns on LST (Fattah et al., 2021a); Oderinde investigated the relationship between carbon dioxide emissions and surface temperature (LST) in ecoregions (Oderinde, 2020).

Since small-scale carbon emission data are difficult to obtain directly, previous studies on carbon emissions have primarily focused on the national, provincial, and prefecture-level cities, but counties are the basic unit of national functional zoning, macro-policy formulation, and micro-policy implementation (Long et al., 2021; Nguyen et al., 2021; Xu et al., 2016; Zheng et al., 2019). Guangdong Province has become China's largest economic province, with robust, comprehensive economic competitiveness and financial strength. The continued increase in carbon emissions will result in environmental changes, and LST is an important indicator of urban climate change, so it is of practical significance to explore the relationship between carbon emissions and LST (Halder et al., 2021; Riahi et al., 2017). Rapid economic growth and urbanization in Guangdong Province inevitably lead to a high concentration of energy consumption, which significantly increases CO₂ emissions. To cope with the enormous pressure of emission reduction and promote the sustainable development of cities, scientifically and accurately describing the temporal and spatial changes of carbon emissions and revealing the interaction mechanism between them and surface temperature are important prerequisites for formulating emission reduction policies tailored to local conditions. In summary, this study examines the response characteristics between carbon emissions and LST and the influencing factors of carbon emissions using land use, carbon emission, LST, and socioeconomic data, over the Guangdong Province, from 2000 to 2017, at the county level. The results are expected to provide data support and theoretical reference to realize the emission reduction measures in Guangdong.

2. Materials and methods

2.1. Study area

Guangdong Province is located in the southern Nanling Mountains, along the South China Sea coast, bordering Guangxi, Hunan, Jiangxi, Fujian, Hong Kong, and Macau, and facing Hainan across the Qiongzhou Strait. It is the most economically developed province in China for nearly 30 years, with its total economic volume accounting for about 1/8th of the country's total. The province experiences a subtropical monsoon climate, along the South China Sea coast, so it has the most abundant light, heat, and water resources in China. It has long summer and warm winter, abundant rainfall, long rainy season, more typhoons and rainstorms in summer and autumn, and occasionally cold air invasion in winter and spring (Li et al., 2021c).

Since solar radiation is the primary heat source influencing LST, an area's latitudinal position significantly impacts its LST (Li et al., 2016). Therefore, this study excluded the two cities with the lowest latitude in southwestern Guangdong Province, Zhanjiang City ($20^{\circ} \sim 21^{\circ}35'N$) and Maoming City ($21^{\circ}22' \sim 22^{\circ}42'N$) (Fig. 1). We selected 108 counties and districts of 19 cities in Guangdong Province, including 2 sub-provincial cities, Guangzhou and Shenzhen.

2.2. Data sources and methods

2.2.1. Data sources

Based on the research needs and availability of information, this study used data about administrative divisions, land use, LST, carbon emission, and socioeconomics, as shown in Table 1.

2.2.2. Research methods

The county-level carbon emission numbers were derived from the China Carbon Accounting Database (CEADs), which estimated carbon dioxide emissions from 2735 counties in China from 1997 to 2017 (Chen et al., 2020; Yong et al., 2022). The database uses the particle swarm optimization-backpropagation (PSO-BP) algorithm to unify the scale of the Defense Meteorological Satellite Program/Operational Linescan System (DMSP/OLS) and National Polar-orbiting Partnership/Visible Infrared Imaging Radiometer (NPP/VIIRS) satellite images. Following the scope of the study area selected in this study (Fig. 1), we chose 19 cities in Guangdong Province (excluding Zhanjiang and Maoming cities), including 108 counties, to investigate the response characteristics of LST and carbon emissions.

The MOD11A2 LST data was obtained from LAADS DAAC. The MOD11A2 LST data is a data product with a resolution of 1KM and a recording interval of 8 days. First, the downloaded LST data was preprocessed by reprojection and format conversion using the MODIS Reprojection Tool. The study area was cropped in ArcGIS, although MOD11A2 is an eight-day synthetic product, there are still missing values due to weather cloudiness, so this study removed the outliers and averaged the data. Then, the band operation method used

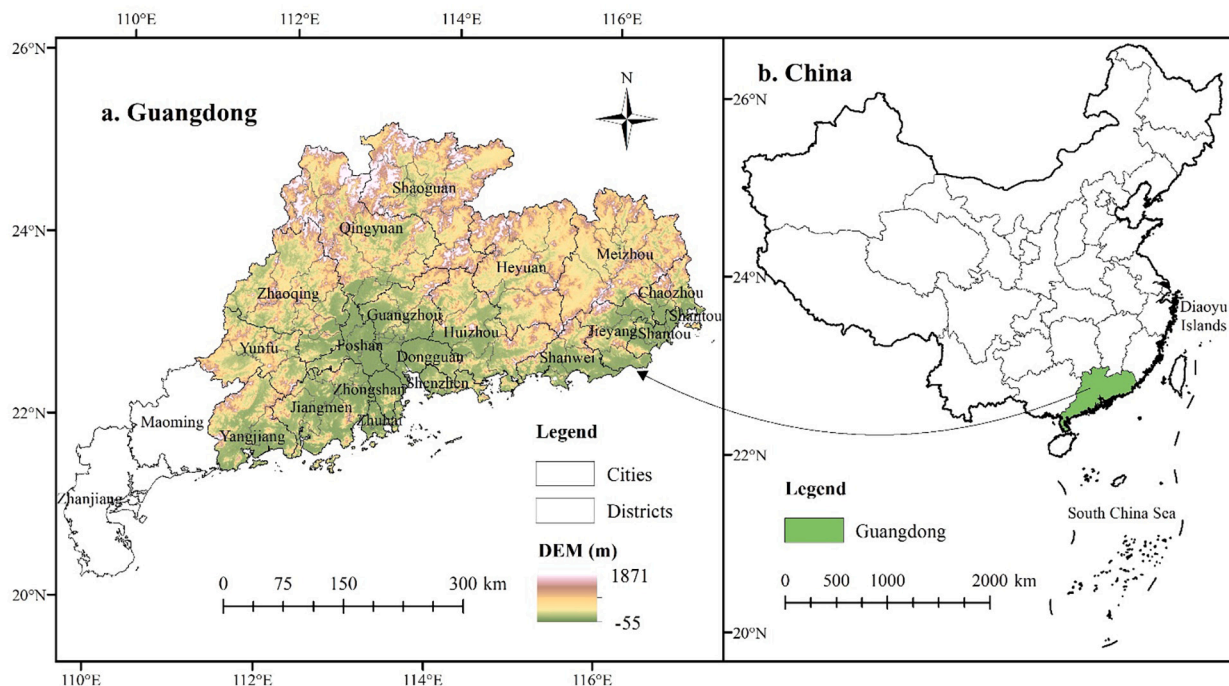


Fig. 1. Location of study area.

Table 1
Data sources and descriptions.

Type of data	Resolution	Time/Year	Data sources
Administrative division data	–	–	https://www.webmap.cn/commres.do?method=dataDownload
Dem	90 m	–	http://www.gscloud.cn/
Land use data	30 m	2000, 2005, 2010, 2017	https://zenodo.org/record/4417810#.Yozchflynhc
MOD11A2	1000 m	2000, 2005, 2010, 2017	https://ladsweb.modaps.eosdis.nasa.gov/
Carbon emissions data	–	2000, 2005, 2010, 2017	https://www.ceads.net.cn/data/county/
Guangdong Statistical Yearbook, China	–	2000, 2005, 2010, 2017	https://www.cnki.net/
County Statistical Yearbook	–	2000, 2005, 2010, 2017	https://www.cnki.net/

Field Calculator in ArcGIS to obtain the annual average, annual average daytime, and annual average nighttime LST data. Finally, the image pixel value of MOD11A2 was converted to degrees Celsius by using ArcGIS software (digital numbers [DNs]) (Wang and Jing, 2015); the calculation formula is as follows:

$$LST (^{\circ}C) = DN \times 0.02 - 273.15 \tag{1}$$

Where DN is the brightness temperature of the MOD11A2 image.

The land use data were acquired from the National Key Experiment of Surveying, Mapping, and Remote Sensing Information Engineering of Wuhan University. Using Landsat images on Google Earth Engine, the annual land cover product of China (CLCD) from 1985 to 2019 was constructed. The training samples were collected by combining stable samples drawn from the Chinese land use/cover dataset (CLUD) and visual interpretation samples from the Landsat satellite time-series data, Google Earth, and Google Maps. Several temporal metrics are constructed from all available Landsat data and fed to a random forest classifier to obtain classification results. Further, a post-processing method combining spatiotemporal filtering and logical reasoning is proposed to improve the spatiotemporal consistency of CLCD (Yang and Huang, 2021). This study uses ArcGIS software to analyze the influencing factors of carbon emissions by extracting water and impervious surface area.

Spearman correlation analysis: This method is suitable for non-continuous data or when the overall distribution of variables is unknown (Schober et al., 2018). Considering that the carbon emission data does not conform to a normal distribution, Spearman correlation analysis is selected to test the correlation between LST data and carbon emission data. Its calculation formula is as follows:

$$r_s = \frac{\sum_{i=1}^n (r_i - \bar{r})(s_i - \bar{s})}{\sqrt{\sum_{i=1}^n (r_i - \bar{r})^2} \sqrt{\sum_{i=1}^n (s_i - \bar{s})^2}} \tag{2}$$

In the formula: r_i and s_i represent the ranks of x_i and y_i respectively. When an equal value appears in the variable, the rank corresponding to the value is the average of the ranks corresponding to these values. The value range of r_s is $[-1, 1]$, $r_s=1$ means that one variable increases monotonically with another variable; $r_s=-1$ means that one variable monotonically decreases with another variable.

Geodetector: The geodetector model is a statistical method for detecting spatial heterogeneity and revealing the effects of driving factors, and its model has the advantages of less limited sample size and good at handling types and quantities (Wang and Xu, 2017). However, the endogeneity and collinearity of carbon emission influencing factors are serious, and the geographic detector principle ensures immunity to the collinearity of independent variables (Xu et al., 2021). This study used factor detection and interaction detection in geographic detectors to reveal the impact of different factors and their interactions on carbon emissions. Factor detection is measured by the q -value, which is expressed as:

$$q = 1 - \frac{\sum_{h=1}^L N_h \sigma_h^2}{N \sigma^2} \tag{3}$$

In the formula: h is the number of layers of the variable, $h = 1, \dots, L$; N_h and σ_h^2 are the sample size and variance of the h th layer; N and σ^2 are the sample size and variance. q is the explanatory degree of the detection factor to carbon emissions, and the value range is $[0, 1]$. The larger the q value, the stronger the explanatory power of the factor to carbon emissions, and vice versa.

The primary objective of interaction detection is to identify the interaction between different factors affecting carbon emissions,

Table 2
Interaction types and discrimination basis of geodetector.

Interaction type	Judgment basis
Two-factor enhancement	$q(X1 \cap X2) > \text{Max}[q(X1), q(X2)]$
Nonlinear enhancement	$q(X1 \cap X2) > q(X1) + q(X2)$
Nonlinear weakening	$q(X1 \cap X2) < \text{Min}[q(X1), q(X2)]$
One-Factor Nonlinear Attenuation	$\text{Min}[q(X1), q(X2)] < q(X1 \cap X2) < \text{Max}[q(X1), q(X2)]$
Independent	$q(X1 \cap X2) = q(X1) + q(X2)$

that is, to evaluate whether each factor will enhance or weaken the explanatory power of carbon emissions when they act together in pairs. The relationship between the two factors includes five types: nonlinear weakening, single-factor nonlinear weakening, two-factor enhancement, independence, and nonlinear enhancement. The strength and type of factor interaction are shown in Table 2:

Following the existing research and data availability (Balsalobre-Lorente et al., 2018; Li et al., 2021d; Song et al., 2014), this study selects eight indicators to discuss the influencing factors of carbon emissions as follows: economic aggregate (GRP), population size (PS), economic density (ED), industrial structure (IS), government intervention (GI), water resources (WR), land scale (LS), and land intensity (LI). The specific expression methods are shown in Table 3.

3. Results

3.1. Spatiotemporal differentiation of carbon emissions

Humans generate a large amount of CO₂ in production activities. Therefore, understanding the spatial and temporal differentiation characteristics of carbon emissions can provide important guidance for the purposeful suppression and reduction of carbon emissions and the improving human settlements.

Fig. 2 shows the spatiotemporal distribution of carbon emissions in a million tons (10Mt) across the Guangdong Province in 2000, 2005, 2010, and 2017. As shown in Fig. 2, the total amount of carbon emissions from 2000 to 2017 has a significantly increasing trend and presents a semi-circular layered structure. The areas with significant carbon emissions are concentrated in southern Zhongshan, Dongguan, Guangzhou, and some counties in Shenzhen. The areas showing rapid growth of carbon emission are also the regions with a large carbon emission footprint that show a trend of expansion, including cities like Dongguan, Zhongshan, Guangzhou, Shenzhen, Huizhou, and Foshan.

In 2000, only Dongguan City and Zhongshan City had >10 Mt. of carbon emissions, and nearly half of the counties and districts had yearly carbon emissions of <1 Mt. In 2005, Dongguan's annual carbon emissions reached 34.328 Mt., far ahead of other regions. The number of cities and counties with >10 Mt. increased to 5 (Dongguan, Zhongshan, Nanhai District, Shunde District of Foshan, and Bao'an District of Shenzhen). In 2010, the carbon emissions of Dongguan and Zhongshan exceeded 20 Mt., and the carbon emissions of 8 counties exceeded 10 Mt. By 2017, the carbon emissions of 12 counties exceeded 10 Mt., and few counties had annual carbon emissions of <1 Mt.

3.2. Spatiotemporal differentiation of LST

Fig. 3 shows the spatiotemporal distribution of the annual average LST for the Guangdong Province between 2000 and 2017. The annual average LST varies between 17 and 24 °C for all the time series, with the highest temperatures distributed in Guangzhou, Dongguan, Shenzhen, and Foshan areas. The annual average LST in 2000 is higher than that of the other three years. This may be due to the remarkable effect of returning farmland to a forest in Guangdong Province after 2000 because afforestation has a strong net cooling effect, and the frequency and intensity of rainfall in Guangdong Province in 2000 are also the smallest (Li et al., 2021d; Shen et al., 2019). The annual average LST in 2005 was still higher than in 2010 and 2017 for most regions. The annual average LST in 2010 was generally lower, while those in 2017 were higher. Fig. 4 shows the spatiotemporal distribution of the annual average daytime LST. The annual average daytime LST is consistent with the annual average LST change. The difference is that the annual average daytime LST is mainly 21–28 °C. Fig. 5 shows the spatiotemporal distribution of the annual average nighttime LST. Similarly, the annual average nighttime LST is consistent with the annual average LST change, and the annual average nighttime LST is mainly 13–20 °C.

3.3. Response characteristics of carbon emissions and LST

The obtained annual average, annual average daytime, and annual average nighttime LST data are separately counted, and then the normality test is carried out on the LST data and carbon emission data. Since the carbon emission data does not conform to the normal distribution, the Spearman correlation analysis was selected to test the correlation between LST data and carbon emission data. The correlation results are shown in Table 4:

Table 4 shows a positive correlation between total carbon emissions and LST, with a correlation coefficient between 0.3 and 0.7. Overall, the highest LST has a higher correlation with the total carbon emissions, and the lowest LST has a lower correlation with the

Table 3
Index calculation.

Index	Calculation method
Economic aggregate (GRP)	Gross Regional Product
Population size (PS)	Population
Economic density (ED)	GRP/Population
Industrial structure (IS)	Secondary Industry Output Value/GRP
Government intervention (GI)	Fiscal Expenditure/GRP
Water resources (WR)	Water area
Land scale (LS)	Impervious surface area
Land intensity (LI)	Impervious surface/county area

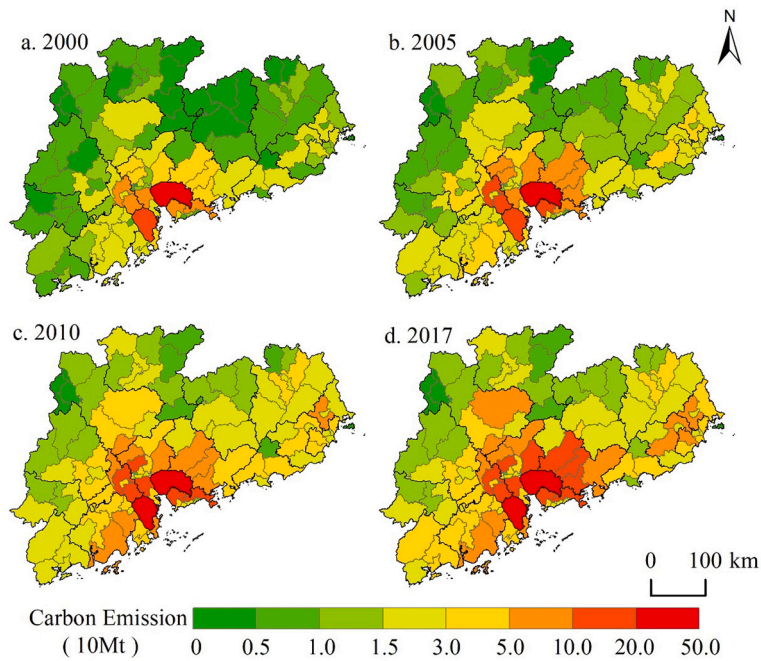


Fig. 2. Spatiotemporal distribution of carbon emissions in the Guangdong Province between 2000 and 2017: (a)2000, (b) 2005, (c) 2010, (d) 2017.

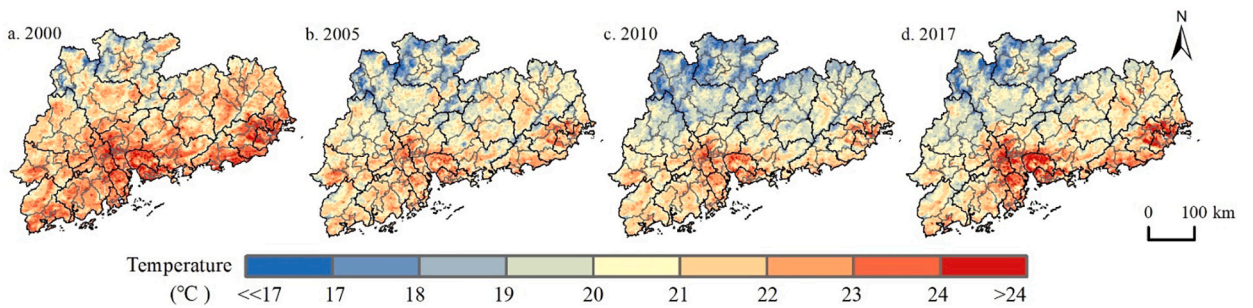


Fig. 3. Spatiotemporal distribution of annual average LST: (a) 2000, (b) 2005, (c) 2010, (d) 2017.

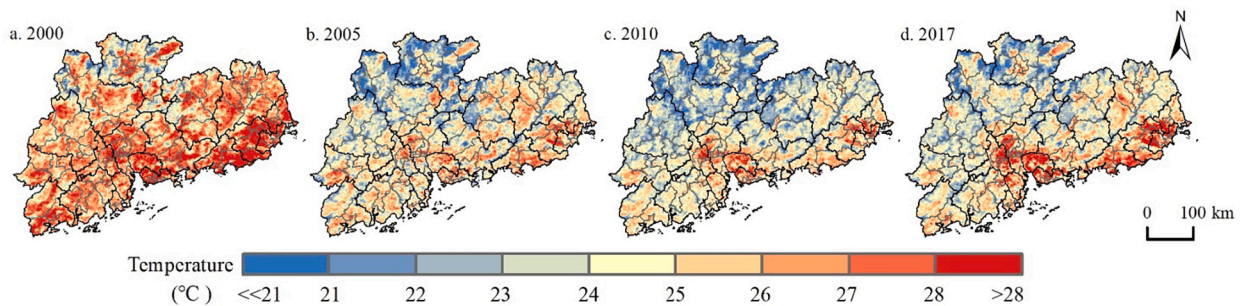


Fig. 4. Spatiotemporal distribution of annual average daytime LST: (a) 2000, (b) 2005, (c) 2010, (d) 2017.

total carbon emissions. The correlation coefficient between carbon emissions and LST in 2000 was generally higher than that of the other three years in 2005, 2010, and 2017, which is consistent with the spatiotemporal differentiation of LST in 3.2; the temperature in 2000 was higher than that in the other three years. This further demonstrated that increased carbon emissions would lead to a rise in global temperature (Hashimoto, 2019; Solomon et al., 2009). As for the correlation between annual average LST and carbon emissions, annual average LST is greater than annual average daytime LST, and annual average LST is greater than annual average nighttime LST.

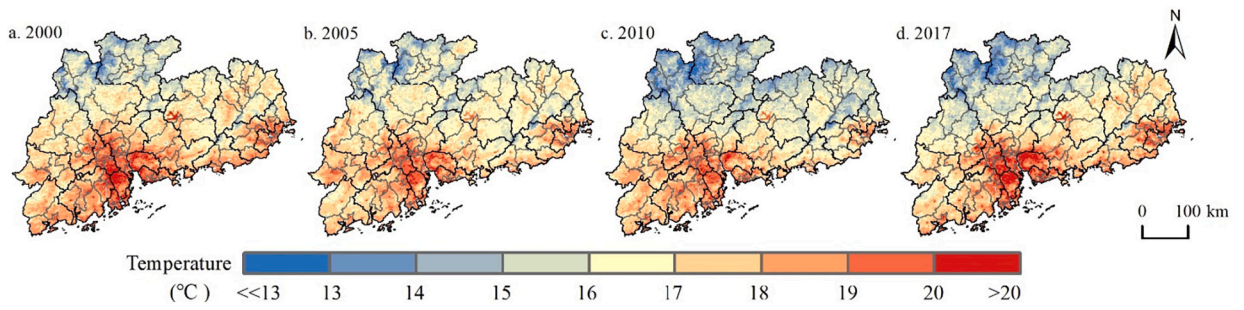


Fig. 5. Spatiotemporal distribution of annual average nighttime LST: (a) 2000, (b) 2005, (c) 2010, (d) 2017.

Table 4
Correlation between carbon emissions and LST.

Year	Mean	Min	Max	Day_mean	Day_min	Day_max	Night_mean	Night_min	Night_max
2000	0.622**	0.443**	0.666**	0.535**	0.414**	0.406**	0.602**	0.455**	0.689**
2005	0.581**	0.412**	0.666**	0.529**	0.332**	0.560**	0.519**	0.428**	0.666**
2010	0.561**	0.390**	0.693**	0.552**	0.383**	0.601**	0.533**	0.386**	0.689**
2017	0.547**	0.378**	0.647**	0.521**	0.344**	0.534**	0.531**	0.408**	0.686**

Note: * $P < 0.10$; ** $P < 0.01$.

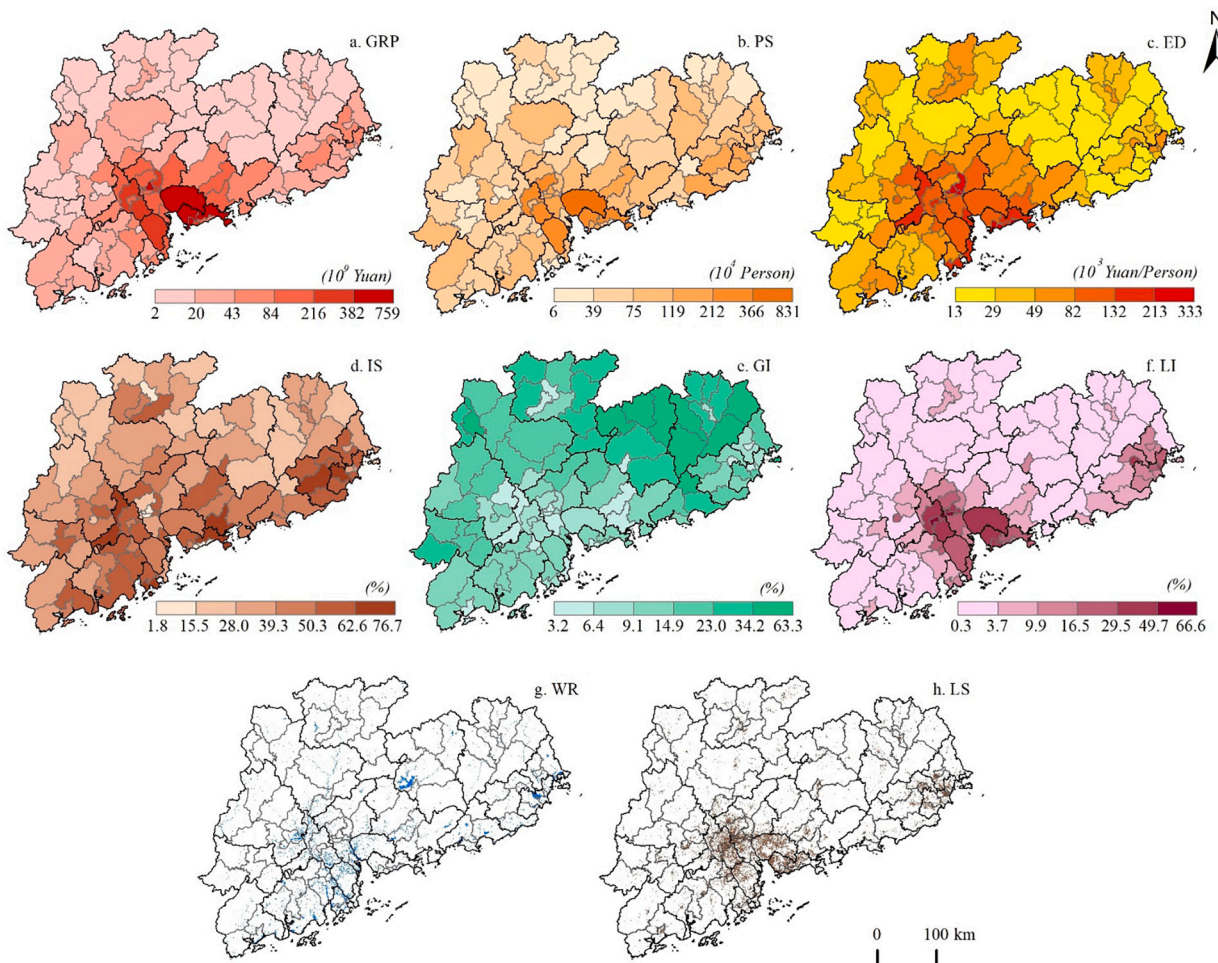


Fig. 6. Spatial distribution of factors affecting carbon emissions: (a) GRP, (b) PS, (c) ED, (d) IS, (e) GI, (f) LI, (g) WR, (h) LS.

For the correlation between the maximum average LST and carbon emissions, the annual average nighttime maximum LST (AANLST_max) is greater than the annual average maximum LST (AALST_max), and AALST_max is greater than annual average daytime maximum LST (AADLST_max). For the correlation between the minimum average temperature and carbon emissions, the annual average nighttime minimum LST (AANLST_min) is greater than the annual average minimum LST (AALST_min), and AALST_min is greater than the annual average daytime minimum LST (AALDST_min). The AALST_min is consistent with the AALST_max, which may be because carbon emissions have a stronger correlation with higher LST. In contrast, at night, the LST is less affected by other factors and thus can show a stronger correlation with carbon emissions (Hu and Brunsell, 2013).

3.4. Influencing factors of carbon emissions

Understanding the temporal and spatial differentiation laws and influencing factors of carbon emissions in Guangdong Province is crucial to the sustainable development, energy conservation, and emission reduction of Guangdong Province.

Eight factors were selected based on existing research results and data availability to estimate their degree of influence on carbon emissions. These factors are economic aggregate (GRP), population size (PS), economic density (ED), industrial structure (IS), government intervention (GI), water resources (WR), land scale (LS), and land intensity (LI), as shown in Fig. 6. This study selects the cross-sectional data of four-time series 2000, 2005, 2010, and 2017 in 108 counties in Guangdong Province. After using the natural discontinuity method and the discretization of the impact factor, the spatial differentiation of carbon emissions was driven by a geographic detector (Cao et al., 2013). The contribution of each factor to carbon emissions and the interactive detection results are shown in Table 5 and Fig. 7.

3.4.1. Single-factor probe results

As shown in Table 5, the leading factors of carbon emissions in Guangdong Province were different in different periods. In 2000 and 2005, GRP had the strongest impact on carbon emissions; in 2010 and 2017, LS had the strongest impact. Overall, GRP, LS, and LI influence the spatial differentiation of carbon emissions is always stronger, followed by ED and WR. The effects of GI, IS, and PS on carbon emissions are relatively weak, the effects of IS and PS on carbon emissions are relatively stable, and the effects of GI and ED on carbon emissions show strong fluctuations.

Economic aggregate (GRP), population size (PS), and economic density (ED): From 2000 to 2017, the influence of GRP gradually weakened, but the overall effect was still very high. The q value ranged from 0.838 to 0.906. The effect of PS was weak and fluctuated continuously. Constrained by GRP and PS, the effect of ED decreased from 0.867 to 0.548, showing a gradually weakening trend. This demonstrated that improving the level of economic development can lead to an increase in carbon emissions. Therefore, regions with better economic growth need to pay attention to the establishment of special technologies for energy conservation, emission reduction and clean development.

Industrial structure (IS) and government intervention (GI): Compared with other influencing factors, the explanatory power of IS and GI on carbon emissions showed a weak influence. Their q-value ranges are 0.286–0.367 and 0.284–0.404, respectively, and the influence of GI had slightly stronger volatility. Optimizing and adjusting the industrial structure can effectively alleviate carbon emissions. Government intervention can influence carbon emissions; the government can guide enterprises to upgrade technology and improve energy efficiency through subsidies and other methods.

Water resources (WR): The q-value of WR ranges from 0.361 to 0.451. Despite the fluctuations, overall, it is relatively stable. This is most likely because the coastal Guangdong Province, with sufficient water sources, has a largely stable influence on carbon emissions.

Land scale (LS) and land intensity (LI): LS and LI are the two factors with stronger explanatory power for carbon emissions among all factors, but the influence of LI is slightly weaker than that of LS. The q values of LS and LI are in the range of 0.876–0.909, 0.777–0.814, respectively, indicating that the impervious surface's size has a significant effect on carbon emissions. Therefore, we should pay full attention to the centralized and efficient use of land and plan the layout rationally to prevent the growth of carbon emissions from endangering the ecological environment of human settlements.

Table 5
Single factor detection results.

Impact factor	q			
	2000	2005	2010	2017
Economic aggregate (GRP)	0.906***	0.894***	0.844***	0.838***
Population size (PS)	0.220**	0.205**	0.180**	0.255**
Economic density (ED)	0.867***	0.548***	0.594***	0.585***
Industrial structure (IS)	0.352***	0.286**	0.367***	0.352***
Government intervention (GI)	0.284***	0.345***	0.388***	0.404***
Water resources (WR)	0.451***	0.424***	0.426***	0.362***
Land scale (LS)	0.880***	0.876***	0.909***	0.882***
Land intensity (LI)	0.814***	0.803***	0.795***	0.777***

Note: *P < 0.10; **P < 0.05; ***P < 0.01.

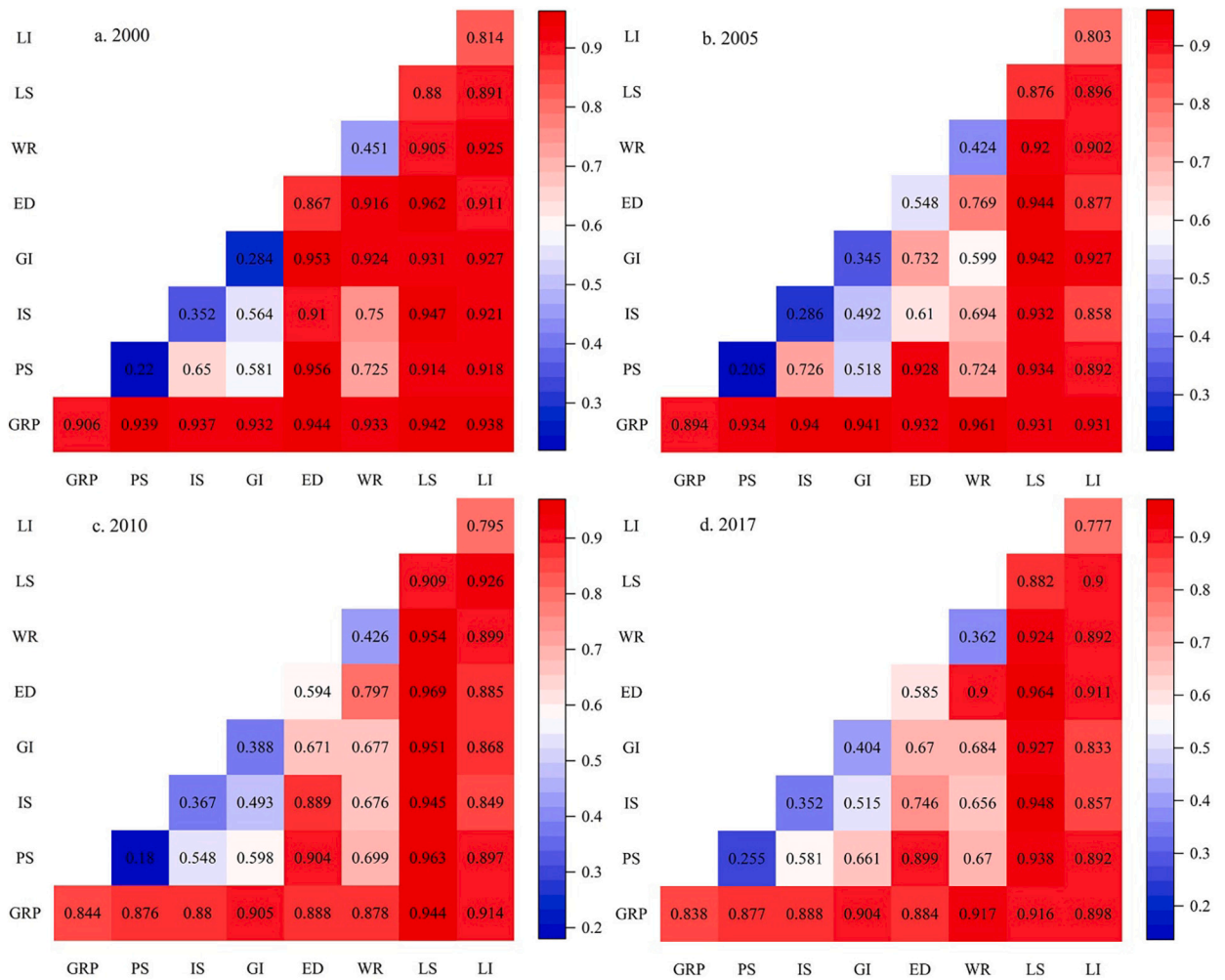


Fig. 7. Results of the factor interaction detection: (a) 2000, (b) 2005, (c) 2010, (d) 2017.

3.4.2. Factor interaction probe results

Factor interaction detection can more specifically detect the effect of two different factors when combined. This study used geographic detectors to conduct pairwise interactive detection of 8 indicators that affect carbon emissions.

Fig. 7 shows the factor interaction detection diagram for the four-time series of 2000, 2005, 2010, and 2017. The results of factor interaction detection are all two-factor enhancement or nonlinear enhancement, and the influence of each factor interaction is greater than that of a single factor. For example, the single-factor detection q-value of PS in 2010 was low, at only 0.18, but the influences of PS∩ED and PS∩LS on carbon emissions were as high as 0.904 and 0.963, respectively. From 2000 to 2017, the interaction between GRP, LS, LI, and other factors was relatively strong, and the interaction detection results were between 0.777 and 0.969; in 2000, the interaction between ED and other factors was also relatively strong, and the interaction detection results were 0.867–0.962; however, from 2005 to 2017, the interactive detection results of ED and other factors declined, and the interaction detection results were 0.548 and 0.932, PS, IS, GI and WR, and other factors have less obvious variation range. The reason is that these factors have the most important influence on carbon emissions, and the interaction effect of factors is more significant than the single factors.

4. Discussion

4.1. Carbon emissions and LST

Economic development and rapid urbanization inevitably increase CO₂ emissions, and the issue of carbon emissions has piqued the interest of scholars. Previous studies on carbon emissions have primarily focused on the national, provincial, and prefecture-level regions. Since the county is China’s fundamental economic space unit and combines macro policy formulation and micro policy implementation (Ang and Su, 2016; Zhang et al., 2020), it is used as the research scale in this study. Determine the impact of different natural and social factors on carbon emissions, which can provide a theoretical reference for the realization of emission reduction

measures in Guangdong.

Previous studies on carbon emissions have been directed towards spatial pattern change characteristics, spatial difference analysis, and the temporal and spatial evolution of carbon emissions (Chen et al., 2021; Zhang et al., 2022). But the latest studies have shown that the carbon emission patterns of land have different degrees of impact on LST (Fattah et al., 2021a; Kafy et al., 2022). There are many related studies on LST, but few have explored the two main bodies' relationship between carbon emissions and LST, further exploring the correlation between carbon emissions and LST. This study elucidates the response characteristics between carbon emissions and LST through long-term panel data. The results show a significant correlation between carbon emissions and LST. The highest average LST has a higher correlation with annual carbon emissions, whereas the average minimum LST has a lower correlation with carbon emissions. For the correlation between carbon emissions and annual average LST, annual average LST is greater than annual average daytime LST, and annual average LST is greater than annual average nighttime LST; for the correlation between carbon emissions and AALST_min/max, AANLST_min/max is greater than AALST_min/max, and AALST_min/max is greater than AADLST_min/max.

4.2. Influencing factors of carbon emissions

Exploring the influencing factors of carbon emissions is of great significance for taking targeted measures to reduce carbon emissions, and then creating sustainable green cities (Sun et al., 2022; Zhao et al., 2021). The results of the study show that the dominant factors of carbon emissions in Guangdong province are different in different periods. In general, GRP, LS and LI have relatively strong explanatory power for carbon emissions (Table 5). It is worth noting that the pairwise interaction of influencing factors has a higher impact on carbon emissions than that of a single factor. This shows that carbon emission is the result of the joint action of multiple factors (Fig. 7). Therefore, setting measures to reduce carbon emissions requires a combination of factors, and targeting only one factor may not work well.

4.3. Limitations

The present study processed data from four years: 2000, 2005, 2010, and 2017. At present, the selection of data has a certain delay. Correlation analysis using the annual average day and night LST data and carbon emission data may mask detailed mechanism changes in the time dimension. Finally, LST results from the joint action of many influencing factors. This study only discusses the correlation between carbon emissions and LST and does not consider and limit other influencing factors, which also causes certain limitations. In the future, we look forward to an in-depth exploration of the correlation between the two at shorter temporal resolutions (such as seasons, day, and night, etc.) and smaller spatial resolutions.

5. Conclusions

The continuous increase in carbon emissions causes environmental changes, and LST is an important indicator for monitoring environmental changes. Therefore, it significance to explore the relationship between carbon emissions and LST and the influencing factors of carbon emissions for sustainable development.

The total amount of carbon emissions showed an increasing trend and a semi-circular layered structure when viewed spatially (Fig. 2). The areas with significant carbon emissions were concentrated in the counties and districts of Zhongshan, Dongguan, Guangzhou, and Shenzhen in the south and show a trend of expansion.

The annual average LST is mainly 17–24 °C, and the high-temperature areas are distributed in Guangzhou, Dongguan, Shenzhen, and Foshan. The annual daytime and nighttime average LST are consistent with the annual average LST change. The annual daytime and nighttime average LST are mainly 21–28 °C and 13–20 °C.

There is a positive correlation between total carbon emissions and LST. The correlation coefficient for the two factors was between 0.3 and 0.7. The highest temperature showed a higher correlation with total carbon emissions, and the lowest temperature exhibited a lower correlation with total carbon emissions.

The dominant factors on carbon emissions were different in the different time periods considered, but the influence of GRP, LS, and LI on the spatial differentiation of carbon emissions were found to be stronger in each time series, followed by ED. The influence of each factor interaction was found to be higher than that of any single factor.

LST result from combination of factors, and the factors that affect surface LST are complex. Therefore, this study only discusses the relationship between carbon emissions and LST and does not comprehensively analyze the effects of other factors. In the future, we look forward to an in-depth exploration of carbon emissions and other influencing factors and comprehensive analysis of LST on smaller time scales and spatial scales.

CRediT authorship contribution statement

Chunrui Song: Data curation, Software, Writing – review & editing. **Jun Yang:** Conceptualization, Methodology, Writing – review & editing. **Feng Wu:** Writing – review & editing. **Xiangming Xiao:** Data curation, Writing – review & editing. **Jianhong Xia:** Writing – review & editing. **Xueming Li:** Writing – review & editing.

Declaration of Competing Interest

This manuscript has not been published or presented elsewhere in part or in entirety and is not under consideration by another journal. We have read and understood your journal's policies, and we believe that neither the manuscript nor the study violates any of these. There are no conflicts of interest to declare.

Data availability

Data will be made available on request.

References

- Acheampong, A.O., Boateng, E.B., 2019. Modelling carbon emission intensity: application of artificial neural network. *J. Clean. Prod.* 225, 833–856. <https://doi.org/10.1016/j.jclepro.2019.03.352>.
- Ang, B.W., Su, B., 2016. Carbon emission intensity in electricity production: a global analysis. *Energy Policy* 94, 56–63. <https://doi.org/10.1016/j.enpol.2016.03.038>.
- Balsalobre-Lorente, D., Shahbaz, M., Roubaud, D., Farhani, S., 2018. How economic growth, renewable electricity and natural resources contribute to CO2 emissions? *Energy Policy* 113, 356–367. <https://doi.org/10.1016/j.enpol.2017.10.050>.
- Cang, D., Chen, C., Chen, Q., Sui, L., Cui, C., 2021. Does new energy consumption conducive to controlling fossil energy consumption and carbon emissions?—evidence from China. *Res. Policy* 74, 102427. <https://doi.org/10.1016/j.resourpol.2021.102427>.
- Cao, W., Yuan, X., 2019. Region-county characteristic of spatial-temporal evolution and influencing factor on land use-related CO2 emissions in Chongqing of China, 1997–2015. *J. Clean. Prod.* 231, 619–632. <https://doi.org/10.1016/j.jclepro.2019.05.248>.
- Cao, F., Ge, Y., Wang, J.-F., 2013. Optimal discretization for geographical detectors-based risk assessment. *Int. J. Geogr. Inf. Sci.* 50, 78–92. <https://doi.org/10.1080/15481603.2013.778562>.
- Cartalis, C., Polydoros, A., Mavrouk, Th., Asimakopoulos, D.N., 2015. Earth observation in support of urban resilience and climate adaptability plans. *TORMSJ* 6, 17–22. <https://doi.org/10.2174/1875413901506010017>.
- Chen, W., Wu, F., Geng, W., Yu, G., 2017. Carbon emissions in China's industrial sectors. *Resour. Conserv. Recycl.* 117, 264–273. <https://doi.org/10.1016/j.resconrec.2016.10.008>.
- Chen, J., Gao, M., Cheng, S., Hou, W., Song, M., Liu, X., Liu, Y., Shan, Y., 2020. County-level CO2 emissions and sequestration in China during 1997–2017. *Sci. Data* 7, 391. <https://doi.org/10.1038/s41597-020-00736-3>.
- Chen, L., Xu, L., Cai, Y., Yang, Z., 2021. Spatiotemporal patterns of industrial carbon emissions at the city level. *Resour. Conserv. Recycl.* 169, 105499. <https://doi.org/10.1016/j.resconrec.2021.105499>.
- Chen, Y., Yang, J., Yang, R., Xiao, X., Xia, J. (Cecilia), 2022. Contribution of urban functional zones to the spatial distribution of urban thermal environment. *Build. Environ.* 216, 109000. <https://doi.org/10.1016/j.buildenv.2022.109000>.
- Cortes, A., Rejuso, A.J., Santos, J.A., Blanco, A., 2022. Evaluating mitigation strategies for urban heat island in Mandaue City using ENVI-met. *J. Urban Manag.* 11, 97–106. <https://doi.org/10.1016/j.jum.2022.01.002>.
- Cui, Y., Xu, X., Dong, J., Qin, Y., 2016. Influence of urbanization factors on surface urban Heat Island intensity: a comparison of countries at different developmental phases. *Sustainability* 8, 706. <https://doi.org/10.3390/su8080706>.
- de Almeida, C.R., Teodoro, A.C., Gonçalves, A., 2021. Study of the Urban Heat Island (UHI) using remote sensing data/techniques: a systematic review. *Environments* 8, 105. <https://doi.org/10.3390/environments8100105>.
- Dong, F., Yu, B., Hadachin, T., Dai, Y., Wang, Y., Zhang, S., Long, R., 2018. Drivers of carbon emission intensity change in China. *Resour. Conserv. Recycl.* 129, 187–201. <https://doi.org/10.1016/j.resconrec.2017.10.035>.
- Dumortier, J., Elobeid, A., 2021. Effects of a carbon tax in the United States on agricultural markets and carbon emissions from land-use change. *Land Use Policy* 103, 105320. <https://doi.org/10.1016/j.landusepol.2021.105320>.
- Eleftheriou, D., Kiachidis, K., Kalmintzis, G., Kalea, A., Bantasis, C., Koumadoraki, P., Spathara, M.E., Tzolaki, A., Tzampazidou, M.I., Gemtzi, A., 2018. Determination of annual and seasonal daytime and nighttime trends of MODIS LST over Greece - climate change implications. *Sci. Total Environ.* 616–617, 937–947. <https://doi.org/10.1016/j.scitotenv.2017.10.226>.
- Fattah, M.A., Morshed, S.R., Morshed, S.Y., 2021a. Multi-layer perceptron-Markov chain-based artificial neural network for modelling future land-specific carbon emission pattern and its influences on surface temperature. *SN Appl. Sci.* 3, 1–22. <https://doi.org/10.1007/s42452-021-04351-8>.
- Ghorbannia, V., Mirsanjari, M., Liaghati, H., Armin, M., 2017. Estimating land surface temperature of land use and land cover in Dena county using single window algorithm and landsat 8 satellite data. *Environ. Sci.* 15, 55–74.
- Gregg, J.S., Andres, R.J., Marland, G., 2008. China: emissions pattern of the world leader in CO₂ emissions from fossil fuel consumption and cement production. *Geophys. Res. Lett.* 35, L08806. <https://doi.org/10.1029/2007GL032887>.
- Halder, B., Bandyopadhyay, J., Banik, P., 2021. Evaluation of the climate change impact on urban Heat Island based on land surface temperature and geospatial indicators. *Int. J. Environ. Res.* 15, 819–835. <https://doi.org/10.1007/s41742-021-00356-8>.
- Hashimoto, K., 2019. Global temperature and atmospheric carbon dioxide concentration. In: *Global Carbon Dioxide Recycling* (Ed.), SpringerBriefs in Energy. Springer Singapore, Singapore, pp. 5–17. https://doi.org/10.1007/978-981-13-8584-1_3.
- He, B.-J., Wang, J., Liu, H., Ulpiani, G., 2021. Localized synergies between heat waves and urban heat islands: implications on human thermal comfort and urban heat management. *Environ. Res.* 193, 110584. <https://doi.org/10.1016/j.envres.2020.110584>.
- He, B.-J., Wang, J., Zhu, J., Qi, J., 2022. Beating the urban heat: Situation, background, impacts and the way forward in China. *Renew. Sust. Energ. Rev.* 161, 112350. <https://doi.org/10.1016/j.rser.2022.112350>.
- Howard, L., 1833. *The Climate of London: Deduced from Meteorological Observations Made in the Metropolis and at Various Places around it*.
- Hu, L., Brunsell, N.A., 2013. The impact of temporal aggregation of land surface temperature data for surface urban heat island (SUHI) monitoring. *Remote Sens. Environ.* 134, 162–174. <https://doi.org/10.1016/j.rse.2013.02.022>.
- Huang, L., Krigsvoll, G., Johansen, F., Liu, Y., Zhang, X., 2018. Carbon emission of global construction sector. *Renew. Sust. Energ. Rev.* 81, 1906–1916. <https://doi.org/10.1016/j.rser.2017.06.001>.
- Kafy, A.-A., Faisal, A.-A., Al Rakib, A., Fattah, Md.A., Rahaman, Z.A., Sattar, G.S., 2022. Impact of vegetation cover loss on surface temperature and carbon emission in a fastest-growing city, Cumilla, Bangladesh. *Build. Environ.* 208, 108573. <https://doi.org/10.1016/j.buildenv.2021.108573>.
- Li, K., Zhang, W., 2021. Directionally and spatially varying relationship between land surface temperature and land-use pattern considering wind direction: a case study in Central China. *Environ. Sci. Pollut. Res.* 28, 44479–44493. <https://doi.org/10.1007/s11356-021-13594-2>.
- Li, Y., Zhao, M., Mildrexler, D.J., Motesharrei, S., Mu, Q., Kalnay, E., Zhao, F., Li, S., Wang, K., 2016. Potential and actual impacts of deforestation and afforestation on land surface temperature: IMPACTS OF FOREST CHANGE ON TEMPERATURE. *J. Geophys. Res. Atmos.* 121, 14,372–14,386. <https://doi.org/10.1002/2016JD024969>.
- Li, Z.-Z., Li, R.Y.M., Malik, M.Y., Murshed, M., Khan, Z., Umar, M., 2021a. Determinants of carbon emission in China: how good is green investment? *Sustain. Prod. Consum.* 27, 392–401. <https://doi.org/10.1016/j.spc.2020.11.008>.
- Li, T., Li, M.-Y., Tian, L., 2021b. Dynamics of carbon storage and its drivers in Guangdong Province from 1979 to 2012. *Forests* 12, 1482. <https://doi.org/10.3390/f12111482>.

- Li, Y., Wang, W., Chang, M., Wang, X., 2021c. Impacts of urbanization on extreme precipitation in the Guangdong-Hong Kong-Macau Greater Bay Area. *Urban Clim.* 38, 100904 <https://doi.org/10.1016/j.uclim.2021.100904>.
- Li, N., Yang, J., Qiao, Z., Wang, Y., Miao, S., 2021d. Urban thermal characteristics of local climate zones and their mitigation measures across cities in different climate zones of China. *Remote Sens.* 13, 1468. <https://doi.org/10.3390/rs13081468>.
- Lin, B., Benjamin, N.I., 2017. Influencing factors on carbon emissions in China transport industry. A new evidence from quantile regression analysis. *J. Clean. Prod.* 150, 175–187. <https://doi.org/10.1016/j.jclepro.2017.02.171>.
- Long, Z., Zhang, Z., Liang, S., Chen, X., Ding, B., Wang, B., Chen, Y., Sun, Y., Li, S., Yang, T., 2021. Spatially explicit carbon emissions at the county scale. *Resour. Conserv. Recycl.* 173, 105706 <https://doi.org/10.1016/j.resconrec.2021.105706>.
- Muchoney, D.M., Strahler, A.H., 2002. Pixel- and site-based calibration and validation methods for evaluating supervised classification of remotely sensed data. *Remote Sens. Environ.* 81, 290–299. [https://doi.org/10.1016/S0034-4257\(02\)00006-8](https://doi.org/10.1016/S0034-4257(02)00006-8).
- Nakata-Osaki, C.M., Souza, L.C.L., Rodrigues, D.S., 2018. THIS – tool for Heat Island simulation: a GIS extension model to calculate urban heat island intensity based on urban geometry. *Comput. Environ. Urban Syst.* 67, 157–168. <https://doi.org/10.1016/j.compenvurbysys.2017.09.007>.
- Nguyen, D.K., Huynh, T.L.D., Nasir, M.A., 2021. Carbon emissions determinants and forecasting: evidence from G6 countries. *J. Environ. Manag.* 285, 111988 <https://doi.org/10.1016/j.jenvman.2021.111988>.
- Norman, J.M., Kustas, W.P., Humes, K.S., 1995. Source approach for estimating soil and vegetation energy fluxes in observations of directional radiometric surface temperature. *Agricultural and Forest Meteorology, Thermal Remote Sensing of the Energy and Water Balance over Vegetation* 77, 263–293. [https://doi.org/10.1016/0168-1923\(95\)02265-Y](https://doi.org/10.1016/0168-1923(95)02265-Y).
- Oderinde, F.O., 2020. A Nexus between Carbon Emissions and Land Surface Temperature in the Six Ecological Zones of Nigeria, 46, p. 16.
- Parvez, I.M., Aina, Y.A., Balogun, A.-L., 2021. The influence of urban form on the spatiotemporal variations in land surface temperature in an arid coastal city. *ISPRS Int. J. Geo-Inf.* 10, 640–659. <https://doi.org/10.1080/10106049.2019.1622598>.
- Rahaman, Z.A., Kafy, A.-A., Saha, M., Rahim, A.A., Almulhim, A.I., Rahaman, S.N., Fattah, Md.A., Rahman, M.T., Selvakumar, K., Faisal, A.-A., Al Rakib, A., 2022. Assessing the impacts of vegetation cover loss on surface temperature, urban heat island and carbon emission in Penang city, Malaysia. *Build. Environ.* 222, 109335 <https://doi.org/10.1016/j.buildenv.2022.109335>.
- Ren, Z., Li, Z., Wu, F., Ma, H., Xu, Z., Jiang, W., Wang, S., Yang, J., 2022. Spatiotemporal evolution of the urban thermal environment effect and its influencing factors: a case study of Beijing, China. *IJGI* 11, 278. <https://doi.org/10.3390/ijgi11050278>.
- Riahi, K., van Vuuren, D.P., Kriegler, E., Edmonds, J., O'Neill, B.C., Fujimori, S., Bauer, N., Calvin, K., Dellink, R., Fricko, O., Lutz, W., Popp, A., Cuaresma, J.C., Kc, S., Leimbach, M., Jiang, L., Kram, T., Rao, S., Emmerling, J., Ebi, K., Hasegawa, T., Havlik, P., Humenöder, F., Da Silva, L.A., Smith, S., Stehfest, E., Bosetti, V., Eom, J., Gernaat, D., Masui, T., Rogelj, J., Strefler, J., Drouot, L., Krey, V., Luderer, G., Harmsen, M., Takahashi, K., Baumstark, L., Doelman, J.C., Kainuma, M., Klimont, Z., Marangoni, G., Lotze-Campen, H., Obersteiner, M., Tabeau, A., Tavoni, M., 2017. The shared socioeconomic pathways and their energy, land use, and greenhouse gas emissions implications: an overview. *Glob. Environ. Chang.* 42, 153–168. <https://doi.org/10.1016/j.gloenvcha.2016.05.009>.
- Rongali, G., Keshari, A.K., Gosain, A.K., Khosra, R., 2018. Split-window algorithm for retrieval of land surface temperature using Landsat 8 thermal infrared data. *J. Geovis spat anal* 2, 1–19. <https://doi.org/10.1007/s41651-018-0021-y>.
- Schober, P., Boer, C., Schwarte, L.A., 2018. Correlation coefficients: appropriate use and interpretation. *Anesth. Analg.* 126, 1763–1768. <https://doi.org/10.1213/ANE.0000000000002864>.
- Sekertekin, A., Zadbagher, E., 2021. Simulation of future land surface temperature distribution and evaluating surface urban heat island based on impervious surface area. *Ecol. Indic.* 122, 107230 <https://doi.org/10.1016/j.ecolind.2020.107230>.
- Shen, W., Li, M., Huang, C., He, T., Tao, X., Wei, A., 2019. Local land surface temperature change induced by afforestation based on satellite observations in Guangdong plantation forests in China. *Agric. For. Meteorol.* 276–277, 107641 <https://doi.org/10.1016/j.agrformet.2019.107641>.
- Shi, Z., Yang, J., Zhang, Y., Xiao, X., Xia, J.C., 2022. Urban ventilation corridors and spatiotemporal divergence patterns of urban heat island intensity: a local climate zone perspective. *Environ. Sci. Pollut. Res.* 1–13 <https://doi.org/10.1007/s11356-022-21037-9>.
- Solomon, S., Plattner, G.-K., Knutti, R., Friedlingstein, P., 2009. Irreversible climate change due to carbon dioxide emissions. *Proc. Natl. Acad. Sci. U. S. A.* 106, 1704–1709. <https://doi.org/10.1073/pnas.0812721106>.
- Song, J., Song, Q., Zhang, D., Lu, Y., Luan, L., 2014. Study on influencing factors of carbon emissions from energy consumption of Shandong Province of China from 1995 to 2012. *Sci. World J.* 2014, 1–12. <https://doi.org/10.1155/2014/684796>.
- Sun, X., Zhang, H., Ahmad, M., Xue, C., 2022. Analysis of influencing factors of carbon emissions in resource-based cities in the Yellow River basin under carbon neutrality target. *Environ. Sci. Pollut. Res.* 29, 23847–23860. <https://doi.org/10.1007/s11356-021-17386-6>.
- Wagner, M., Viswanathan, V., Pelzer, D., Berger, M., Aydt, H., 2015. Cellular automata-based anthropogenic heat Simulation1. *Procedia computer science, international conference on computational science. ICCS 2015 (51)*, 2107–2116. <https://doi.org/10.1016/j.procs.2015.05.480>.
- Waheed, R., Sarwar, S., Wei, C., 2019. The survey of economic growth, energy consumption and carbon emission. *Energy Rep.* 5, 1103–1115. <https://doi.org/10.1016/j.egy.2019.07.006>.
- Wang, Y., Jing, J., 2015. Characteristics of Urban Heat Island Distribution in Guangxi Beibu Gulf Economic Zone Based on MOD11A2 8.
- Wang, X., Li, Y., 2016. Predicting urban heat island circulation using CFD. *Build. Environ.* 99, 82–97. <https://doi.org/10.1016/j.buildenv.2016.01.020>.
- Wang, J., Xu, C., 2017. Principle and prospect of geodetector. *Acta Geographica* 72, 116–134. <https://doi.org/10.11821/dlxb201701010>.
- Wang, Y., Du, H., Xu, Y., Lu, D., Wang, X., Guo, Z., 2018. Temporal and spatial variation relationship and influence factors on surface urban heat island and ozone pollution in the Yangtze River Delta, China. *Sci. Total Environ.* 631–632, 921–933. <https://doi.org/10.1016/j.scitotenv.2018.03.050>.
- Wang, Y., Niu, Y., Li, M., Yu, Q., Chen, W., 2022. Spatial structure and carbon emission of urban agglomerations: spatiotemporal characteristics and driving forces. *Sustain. Cities Soc.* 78, 103600 <https://doi.org/10.1016/j.scs.2021.103600>.
- Xu, S.-C., He, Z.-X., Long, R.-Y., Chen, H., Han, H.-M., Zhang, W.-W., 2016. Comparative analysis of the regional contributions to carbon emissions in China. *J. Clean. Prod.* 127, 406–417. <https://doi.org/10.1016/j.jclepro.2016.03.149>.
- Xu, L., Yu, G., He, N., 2019. Increased soil organic carbon storage in Chinese terrestrial ecosystems from the 1980s to the 2010s. *J. Geogr. Sci.* 29, 49–66. <https://doi.org/10.1007/s11442-019-1583-4>.
- Xu, L., Du, H., Zhang, X., 2021. Driving forces of carbon dioxide emissions in China's cities: an empirical analysis based on the geodetector method. *J. Clean. Prod.* 287, 125169 <https://doi.org/10.1016/j.jclepro.2020.125169>.
- Yang, J., Huang, X., 2021. 30 m annual land cover and its dynamics in China from 1990 to 2019. *Earth Syst. Sci. Data Discuss* 1–29. <https://doi.org/10.5194/essd-2021-7>.
- Yang, J., Zhan, Y., Xiao, X., Xia, J.C., Sun, W., Li, X., 2020. Investigating the diversity of land surface temperature characteristics in different scale cities based on local climate zones. *Urban Clim.* 34, 100700 <https://doi.org/10.1016/j.uclim.2020.100700>.
- Yang, J., Ren, J., Sun, D., Xiao, X., Xia, J.(Cecilia), Jin, C., Li, X., 2021a. Understanding land surface temperature impact factors based on local climate zones. *Sustain. Cities Soc.* 69, 102818 <https://doi.org/10.1016/j.scs.2021.102818>.
- Yang, J., Wang, Y., Xue, B., Li, Y., Xiao, X., Xia, J. (Cecilia), He, B., 2021b. Contribution of urban ventilation to the thermal environment and urban energy demand: different climate background perspectives. *Sci. Total Environ.* 795, 148791 <https://doi.org/10.1016/j.scitotenv.2021.148791>.
- Yang, J., Yang, Y., Sun, D., Jin, C., Xiao, X., 2021c. Influence of urban morphological characteristics on thermal environment. *Sustain. Cities Soc.* 72, 103045 <https://doi.org/10.1016/j.scs.2021.103045>.
- Yong, Z., Li, K., Xiong, J., Cheng, W., Wang, Z., Sun, H., Ye, C., 2022. Integrating DMSP-OLS and NPP-VIIRS nighttime light data to evaluate poverty in southwestern China. *Remote Sens.* 14, 600. <https://doi.org/10.3390/rs14030600>.
- Zhang, X., Xu, M., 2020. Assessing the effects of photovoltaic powerplants on surface temperature using remote sensing techniques. *Remote Sens.* 12, 1825. <https://doi.org/10.3390/rs12111825>.
- Zhang, H., Sun, X., Wang, W., 2017. Study on the spatial and temporal differentiation and influencing factors of carbon emissions in Shandong province. *Nat. Hazards* 87, 973–988. <https://doi.org/10.1007/s11069-017-2805-7>.

- Zhang, Y., Li, S., Luo, T., Gao, J., 2020. The effect of emission trading policy on carbon emission reduction: evidence from an integrated study of pilot regions in China. *J. Clean. Prod.* 265, 121843 <https://doi.org/10.1016/j.jclepro.2020.121843>.
- Zhang, C., Zhao, L., Zhang, H., Chen, M., Fang, R., Yao, Y., Zhang, Q., Wang, Q., 2022. Spatial-temporal characteristics of carbon emissions from land use change in Yellow River Delta region, China. *Ecol. Indic.* 136, 108623 <https://doi.org/10.1016/j.ecolind.2022.108623>.
- Zhao, K., Cui, X., Zhou, Z., Huang, P., Li, D., 2021. Exploring the dependence and influencing factors of carbon emissions from the perspective of population development. *IJERPH* 18, 11024. <https://doi.org/10.3390/ijerph182111024>.
- Zhao, X., Ma, X., Chen, B., Shang, Y., Song, M., 2022. Challenges toward carbon neutrality in China: strategies and countermeasures. *Resour. Conserv. Recycl.* 176, 105959 <https://doi.org/10.1016/j.resconrec.2021.105959>.
- Zhao, Z., Sharifi, A., Dong, X., Shen, L., He, B.-J., 2021. Spatial Variability and Temporal Heterogeneity of Surface Urban Heat Island Patterns and the Suitability of Local Climate Zones for Land Surface Temperature Characterization. *Remote Sens.* 13, 4338. <https://doi.org/10.3390/rs13214338>.
- Zheng, J., Mi, Z., Coffman, D., Milcheva, S., Shan, Y., Guan, D., Wang, S., 2019. Regional development and carbon emissions in China. *Energy Econ.* 81, 25–36. <https://doi.org/10.1016/j.eneco.2019.03.003>.
- Zhong, X., Labeled, J., Zhou, G., Shao, K., Li, Z.-L., 2015. A multi-channel method for retrieving surface temperature for high-emissivity surfaces from hyperspectral thermal infrared images. *Sensors* 15, 13406–13423. <https://doi.org/10.3390/s150613406>.
- Zhou, Y., Chen, M., Tang, Z., Mei, Z., 2021. Urbanization, land use change, and carbon emissions: quantitative assessments for city-level carbon emissions in Beijing-Tianjin-Hebei region. *Sustain. Cities Soc.* 66, 102701 <https://doi.org/10.1016/j.scs.2020.102701>.
- Zou, C., Xiong, B., Xue, H., Zheng, D., Ge, Z., Wang, Y., Jiang, L., Pan, S., Wu, S., 2021. The role of new energy in carbon neutral. *Pet. Explor. Dev.* 48, 480–491. [https://doi.org/10.1016/S1876-3804\(21\)60039-3](https://doi.org/10.1016/S1876-3804(21)60039-3).